Mono- *versus* bidentate coordination of the NONOate $[Et_2N(N_2O_2)]^-$ to copper(II) complexes of tetradentate ligands

Jamie L. Schneider, Jason A. Halfen, Victor G. Young, Jr. and William B. Tolman*

Department of Chemistry and Center for Metals in Biocatalysis, University of Minnesota, 207 Pleasant Street SE, Minneapolis, MN 55455, USA

Copper(II) complexes of $[Et_2N(N_2O_2)]^-$ with tetradentate, tripodal ligands composed of 1,4,7-triazacyclononanes with pyridine (L^{Py}), amide (L^{HAmH}) or phenolate (L^{R2}, R = Me or Bu^t phenolate substituents) groups as the fourth donor were prepared and characterized by spectroscopic and X-ray crystallographic methods. Bidentate *O*,*O*-coordination of $[Et_2N(N_2O_2)]^-$ was observed in the complexes supported by L^{Py} and L^{HAmH}, but the stronger phenolate donor in L^{R2} induced novel monodentate coordination *via* the terminal oxygen atom, defined by X-ray crystallography for R = Bu^t. Comparison of the bonding parameters of $[Et_2N(N_2O_2)]^-$ when bound bidentate *versus* when bound monodentate revealed subtle but significant differences in the N—O distances. The amount and rate of nitric oxide (NO) release from the compounds was measured using a chemiluminescence detection method. Despite the differences in $[Et_2N(N_2O_2)]^-$ structural parameters resulting from the divergent coordination modes, insignificant variation of the rates of NO release therefrom were found.

The extensive biological effector properties and possible pharmacological uses of nitric oxide (NO)[1] and its byproduct peroxynitrite[2] (HOONO) derived from reaction of NO with superoxide (O_2^-) continue to stimulate efforts to develop reagents capable of generating NO under mild conditions for selective delivery to biological targets. Important compounds that readily release NO in aqueous solutions are the diazeniumdiolates ('NONOates'), $[R_2N(N_2O_2)]^-$,[3] the prototype with R = Et (often referred to as DEA/NO) being among the most thoroughly studied.[4] Versions of these molecules that are *O*-alkylated[5] or coordinated to a metal ion[6,7] have been prepared in attempts to modulate their NO release rates. So far, only bidentate coordination of $[Et_2N(N_2O_2)]^-$ *via* its oxygen atoms has been observed in its metal complexes. An analogous metal binding mode also has been observed exclusively for the related species $[RN_2O_2]^-$ (R = alkyl or Ph),[8,9] even when bound to a metalloporphyrin.[10] In copper(II) complexes of $[Et_2N(N_2O_2)]^-$ that only have additional solvate molecules as coligands,[6] the rate of NO release from the bidentate NONOate is unperturbed from that of the simple sodium salt, implicating rapid ligand loss prior to decomposition. We showed recently that a bidentate $[Et_2N(N_2O_2)]^-$ complex of Cu^{II} that is supported by 1,4,7-triisopropyl-1,4,7-triazacyclononane (L^{iPr3}) evolves NO at a slightly slower rate than the sodium salt, thus indicating a modest stabilizing influence of the macrocyclic, multidentate coligand.[7]

In an extension of these studies of the Cu^{II} coordination chemistry of $[Et_2N(N_2O_2)]^-$ in the presence of supporting coligands that may influence its binding mode and the rate of NO release, we decided to use tetradentate ligands of various types in order to force the NONOate to coordinate in a previously unobserved monodentate geometry. Herein we report synthetic, spectroscopic and X-ray crystallographic studies of a series of new complexes of $[Et_2N(N_2O_2)]^-$, including the first example of a complex in which it coordinates *via* a single oxygen atom. In addition, NO evolution rates from these compounds were measured and compared using chemiluminescence detection methods.

Results and Discussion

Syntheses

The macrocyclic ligands with appended pyridyl (L^{Py}),[11] phenolate (L^{R2}, R = Me or Bu^t),[12] and amide (L^{HAmH})[13] arms were chosen because of their demonstrated ability to coordinate to copper ions in tetradentate fashion. They were synthesized as described previously.[11–13] The preparations of the complexes of $[Et_2N(N_2O_2)]^-$ involved either low-temperature metathesis of the sodium salt with the appropriate macrocycle-supported copper(II) chloride complex or, in the case of the amide-appended ligand L^{HAmH}, *in situ* low-temperature assembly of the sodium salt, $CuCl_2$ and L^{HAmH} followed by anion exchange (Scheme 1). The phenoxide starting materials $[L^{R2}CuCl]PF_6$ were reported previously,[12] but compound **1** is new. It was synthesized by mixing L^{Py} with $CuCl_2$ followed by metathesis with NH_4PF_6. Compounds **1**–**4** were isolated in moderate to good yields as crystalline solids, with the exception of **4**, R = Bu^t, which was only obtained in minute quantity, but still sufficient for identification by X-ray crystallography, FTIR, UV/VIS and EPR spectroscopies, and electrospray mass spectrometry. All other compounds were

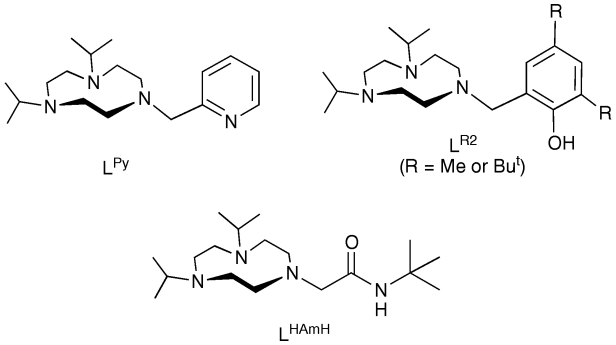

L^{Py} L^{R2} (R = Me or Bu^t) L^{HAmH}

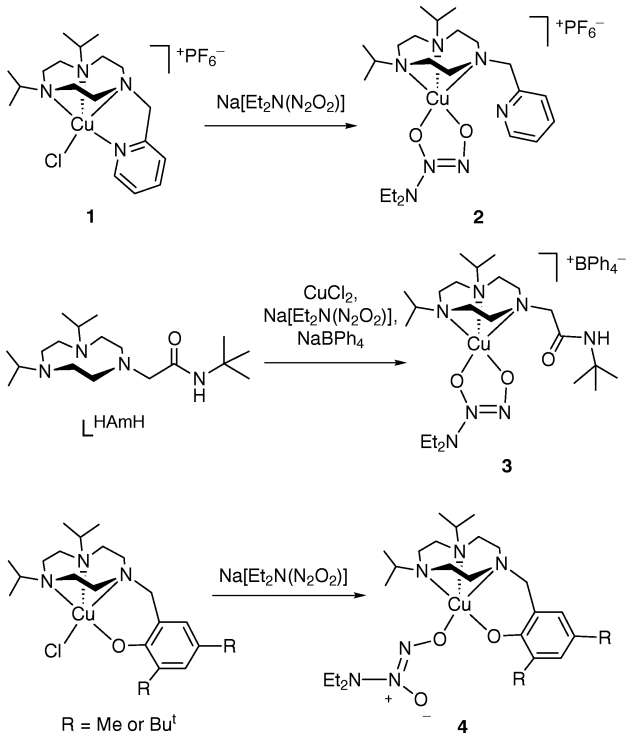

Scheme 1

fully characterized by UV/VIS, FTIR and EPR spectroscopies, elemental analysis (CHN), mass spectrometry (except for **2**) and X-ray crystallography (except for **4**, R = Me).

Structures

Representations of the X-ray crystal structures of **1**–**3** (cationic portions only) and $\mathbf{4}\cdot C_5H_{12}\cdot 0.5C_6H_{12}O_2$ (R = Bu^t, including $C_6H_{12}O_2$ portion) are shown in Fig. 1 and 2. Crystallographic data appears in Table 1 and selected bond distances and angles are listed in Table 2.

The structure of **1** [Fig. 1(a)] reveals binding of all four N donors of the L^{Py} ligand to give a five-coordinate Cu^{II} ion in a geometry intermediate between square pyramidal (sp) and trigonal bipyramidal (tbp); $\tau = 0.46$, where values of 0 and 1 are indicative of rigorous sp and tbp geometries, respectively.[14] This topology is intermediate between the environments of the metal ions in like complexes of the tripod ligands TMPA [tris(methylpyridyl)amine, $\tau = 1.01$, pure tbp], BPQA [bis(methylpyridyl)(methylquinolyl)amine, $\tau = 0.19$, slightly distorted sp] and TMQA [tris(methylquinolyl)amine, $\tau = 0.06$, pure sp] studied by Karlin and coworkers.[15] As noted by Karlin, the often subtle geometric differences between related ligand variants exerts considerable control over Cu^{II} ion structure.

In **2** bidentate coordination of $[Et_2N(N_2O_2)]^-$ *via* its oxygen atoms results in ejection of the soft pyridyl donor of the L^{Py} ligand [Fig. 1(b)]. The oxygen atoms, N(1) and N(4) adopt the equatorial sites and N(7) resides at the axial position [Cu—N(7) = 2.323(3) Å] of the essentially square pyramidal Cu^{II} ion ($\tau = 0.14$), with the pyridine apparently pointing toward the axial vacancy. However, the Cu···N(12) distance is 2.659(3) Å, significantly longer than expected for a bonding interaction, and the nitrogen lone pair is not oriented appropriately for maximum bonding orbital overlap [the pyridine ring plane is displaced from the Cu—N(12) vector]. A similar situation occurs in **3** [Fig. 1(c)], where again $[Et_2N(N_2O_2)]^-$ coordinates in bidentate fashion to the equatorial sites of a Cu^{II} ion in a slightly distorted square pyrimidal coordination

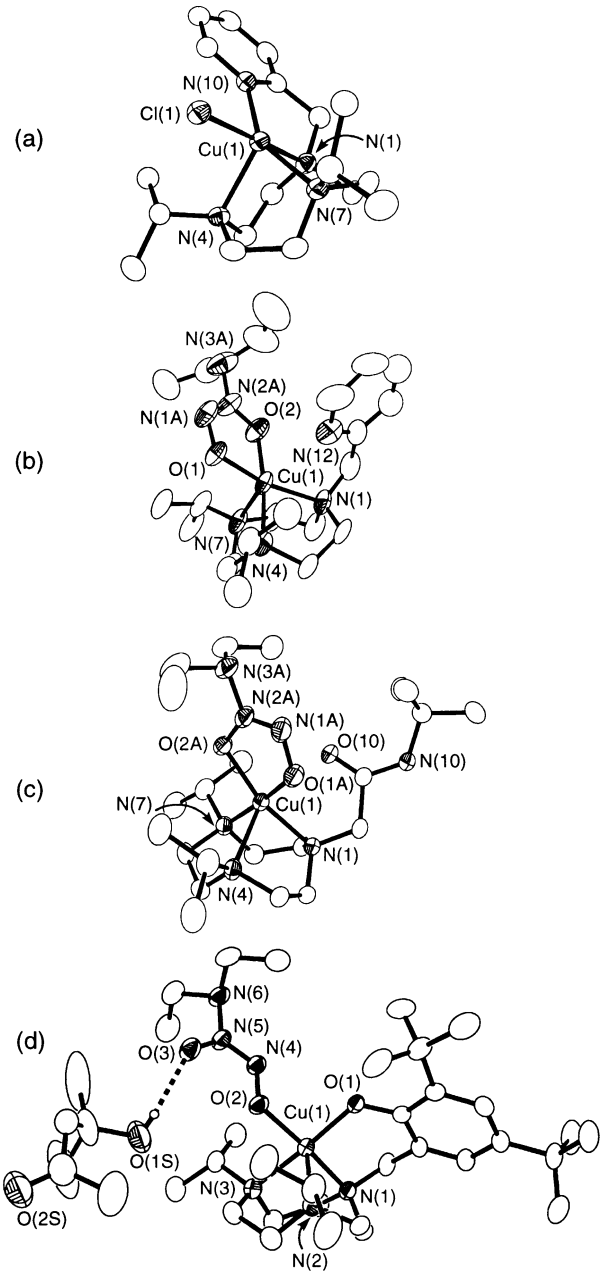

Fig. 1 Representations of the X-ray crystal structures of (a) $[L^{Py}CuCl]PF_6$ (**1**), (b) $\{L^{Py}Cu[Et_2N(N_2O_2)]\}PF_6$ (**2**), (c) $\{L^{HAmH}Cu[Et_2N(N_2O_2)]\}BPh_4$ (**3**) and (d) $\{L^{tBu2}Cu[Et_2N(N_2O_2)]\}\cdot 0.5C_5H_{12}\cdot C_6H_{12}O_2$ [**4** (R = Bu^t)$\cdot 0.5C_5H_{12}\cdot C_6H_{12}O_2$]. For (a)–(c), only the cationic portions are presented, while for (d) the hydrogen-bonded solvate molecule is included. Except for the solvate in (d), only non-hydrogen atoms are shown as 50% ellipsoids

environment ($\tau = 0.20$). While we have found that the amide oxygen binds to the metal in other Cu^{II} complexes of L^{HAmH} and similar amide-appendend ligands,[13] the preference of $[Et_2N(N_2O_2)]^-$ to act as a bidentate chelate and for Cu^{II} to adopt a five-coordinated geometry results in an insignificant interaction between Cu and O(10) [distance = 2.616(2) Å].

The tendency of $[Et_2N(N_2O_2)]^-$ to coordinate in bidentate fashion is finally offset by the strong donor capability of the phenolate arm of the L^{tBu2} ligand in **4** [Fig. 1(d)]. Only the single terminal oxygen atom of $[Et_2N(N_2O_2)]^-$ binds to the copper ion *via* its *anti* lone pair. An essentially perfect square pyramidal geometry is adopted ($\tau = 0.01$) in the complex, with the equatorial positions occupied by the phenolate and $[Et_2N(N_2O_2)]^-$ oxygen donor atoms and the two macrocyclic N donors N(1) and N(3); the third N donor N(2) is axial

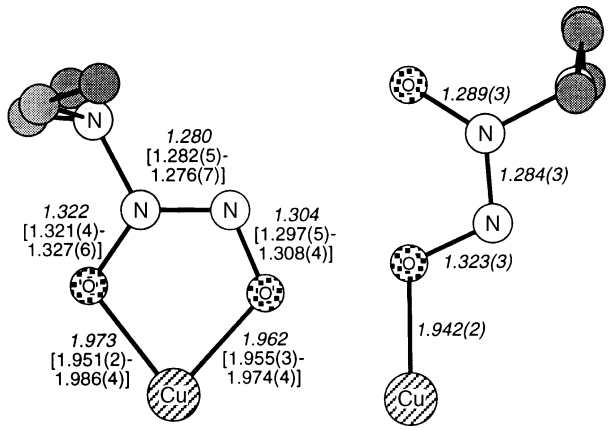

Fig. 2 Comparison of the $\{Cu[Et_2N(N_2O_2)]\}^+$ cores of (left) $\{L^{iPr3}Cu[Et_2N(N_2O_2)]\}O_3SCF_3$,[7] **2** and **3**, and (right) **4** (R = Bu^t). For the bidentate core on the left, average bond lengths are shown in italics with ranges in brackets

[Cu—N(2) = 2.321(3) Å]. As seen in other structures of Cu^{II} complexes of L^{R2},[12] the copper phenolate Cu—O(1) distance is short [1.916(3) Å]. Interestingly, the uncoordinated $[Et_2N(N_2O_2)]^-$ oxygen atom O(3) is hydrogen-bonded [O(3)···O(1S) = 2.055(3) Å] to a solvate molecule identified as 3-hydroxy-3-methyl-2-pentanone, the aldol condensation product of the crystallization cosolvent acetone.

Comparison of the bonding parameters of $[Et_2N(N_2O_2)]^-$ when bound bidentate in $\{L^{iPr3}Cu[Et_2N(N_2O_2)]\}O_3SCF_3$,[7] **2** and **3** *versus* when bound monodentate in **4** reveals subtle but significant differences (Fig. 2). While the Cu—O and N—N distances are congruent among all the compounds, a change in the N—O distances as a function of coordination mode is evident. Thus, in the bidentate compounds the terminal N—O bond length is slightly shorter (ave. ~0.02 Å) than the internal (Et_2N)N—O distance, but in **4** the trend is reversed. An analogous, although even greater, lengthening of the terminal and shortening of the internal (Et_2N)N—O bonds [1.399(4) Å and 1.241(4) Å, respectively] was seen upon regiospecific alkylation of the terminal oxygen of $[Et_2N(N_2O_2)]^-$.[5] Thus, alkylation and monodentate metalation of $[Et_2N(N_2O_2)]^-$ occur with similar regiochemistry (terminal oxygen) and result in similar structural perturbations, mitigated in **4** to some extent presumably because of the strong hydrogen-bonding interaction with the internal oxygen and the less covalent Cu—O (*vs.* C—O) bond.

Spectroscopic properties

Spectral data acquired for **1**–**4** corroborate the X-ray crystallographic results, particularly with respect to the $[Et_2N(N_2O_2)]^-$ binding mode in **2**–**4**. All of the compounds exhibit clean axial X-band EPR spectra consistent with five-coordinate Cu^{II} species. Coordination of $[Et_2N(N_2O_2)]^-$ is indicated by appropriate parent ions in the electrospray mass spectra of **3** and **4** (R = Me and Bu^t) and by intense bands between 250 and 300 nm in the UV/VIS spectra of **2**–**4**, but these data do not allow mono- or bidentate binding to be distinguished. In **3** and **4**, however, spectral features due to the respective amide or phenolate arms are diagnostic of their coordination or lack thereof, which in turn allows the nature of the $[Et_2N(N_2O_2)]^-$ binding to be inferred. The position of the sharp, intense amide carbonyl ('amide I') band in FTIR spectra of complexes of L^{HAmH} indicates whether it is bound to a Cu^{II} ion; when coordinated $\nu_{amide\ I} \approx 1620\ cm^{-1}$, whereas when free it shifts to $\approx 1670\ cm^{-1}$.[13] Observation of this feature at 1679 cm^{-1} for **3** as a KBr pellet confirms the absence of coordination of the amide carbonyl determined crystallographically. In **4**, coordination of the phenolate arm in MeOH solution is evident from the presence of a phenolate → Cu^{II} LMCT at ≈500 nm (ε 500–1000 $M^{-1}\ cm^{-1}$) in UV/VIS spectra.[12] In view of the strong binding capability of the macrocycles in L^{R2} and the evidence for phenolate coordination, we conclude that the monodentate coordination of $[Et_2N(N_2O_2)]^-$ in **4** that was identified in the solid state is retained in solution.

NO evolution

Nitric oxide release from compounds **2**–**4**, as well as $Na[Et_2N(N_2O_2)]$ itself and the previously studied $\{L^{iPr3}Cu[Et_2N(N_2O_2)]\}O_3SCF_3$,[7] was quantitated under two types of acidic conditions (0.1 M HCl and 1.0 M HOAc) and at pH 7.4 (PBS buffer)[16] using chemiluminescence detection.[17] The overall amount of NO released and pseudo-first-order rate constants for NO evolution were determined at 37 °C (Table 3). More accurate determinations of the amount and rate of NO release than possible in previous studies[7] was enabled through the use of a more sensitive instrument with a smaller void volume. As a result, k_{obs} values differed from those determined before with the less sensitive apparatus, particularly when NO generation was fast under acidic conditions.

It is apparent upon consideration of the data in Table 3 that under acidic conditions the NO release rates generally differ insignificantly among the parent $Na[Et_2N(N_2O_2)]$ and the Cu^{II} complexes, except for $\{L^{iPr3}Cu[Et_2N(N_2O_2)]\}O_3SCF_3$ with no NaOH added, which releases NO ≈ 10 times slower in 1.0 M HOAc.[18] Rates of NO generation are slower at pH 7.4 and show some divergences among the different sources, with the slowest rate being from the previously studied $\{L^{iPr3}Cu[Et_2N(N_2O_2)]\}O_3SCF_3$ when 10 mM NaOH was pre-added. Modest stabilization of $[Et_2N(N_2O_2)]^-$ in this complex thus is confirmed. Importantly, however, there does not appear to be any correlation between the structural features of the $\{Cu[Et_2N(N_2O_2)]\}^+$ moiety in the series of complexes and the rate of NO evolution, and there is little, if any, stabilization of $[Et_2N(N_2O_2)]^-$ in the new compounds relative to its sodium salt. Indeed, k_{obs} for **3** is *greater* than for $Na[Et_2N(N_2O_2)]$ at pH 7.4.

Conclusions

Through spectral and X-ray crystallographic studies we have found that bidentate coordination of $[Et_2N(N_2O_2)]^-$ is preferred for selected tetradentate, tripodal ligands composed of 1,4,7-triazacyclononanes with pyridine or amide groups as the fourth donor. When a stronger phenolate ligand is appended to the macrocycle, however, monodentate coordination was accessed and structurally characterized for the first time. Subtle but observable differences in certain bond lengths of $[Et_2N(N_2O_2)]^-$ were found when it is coordinated to Cu^{II} in mono- *versus* bidentate fashion. To our disappointment, and despite changes evident in NONOate structural parameters resulting from divergent coordination modes, the rates of NO release therefrom were found to vary insignificantly among the various compounds. These findings imply that simple coordination chemistry considerations are of limited importance in design efforts aimed at controlling NO release rates by metal–NONOate compounds, at least for those complexes we have studied so far.

Experimental

Unless otherwise noted, all reagents, solvents and gases used were obtained commercially and were of analytical grade.

Table 1 Crystallographic data for **1–4**

	$[L^{Py}CuCl]PF_6$ (**1**)	$\{L^{Py}Cu[Et_2N(N_2O_2)]\}PF_6$ (**2**)	$\{L^{HAmH}Cu[Et_2N(N_2O_2)]\}BPh_4$ (**3**)	$\{L^{tBu2}Cu[Et_2N(N_2O_2)]\}\cdot 0.5\,C_5H_{12}\cdot C_6H_{12}O_2$ (**4**$\cdot 0.5C_5H_{12}\cdot C_6H_{12}O_2$)
Empirical formula	$C_{22}H_{42}CuF_6N_7O_2P$	$C_{22}H_{42}CuF_6N_7O_2P$	$C_{46}H_{68}BCuN_7O_3$	$C_{39.50}H_{76}CuN_6O_5$
M	548.44	645.14	841.42	778.60
Crystal habit, color	plate, blue	block, green	plate, aqua	plate, brown-blue dichroic
Crystal size/mm	0.50 × 0.45 × 0.24	0.45 × 0.25 × 0.22	0.48 × 0.38 × 0.06	0.46 × 0.35 × 0.06
Crystal system	Orthorhombic	Monoclinic	Monoclinic	Monoclinic
Space group	*Pbca*	$P2_1/n$	$P2_1/c$	$P2_1/n$
a/Å	10.3032(2)	8.4217(1)	14.8989(2)	15.7754(2)
b/Å	17.2947(4)	12.6397(2)	13.0847(1)	9.2371(1)
c/Å	25.6681(3)	27.8874(3)	23.3758(2)	31.0991(2)
β/°		94.320(1)	91.523(1)	99.207(1)
U/Å^3	4573.8(2)	2960.12(7)	4555.45(8)	4473.34(8)
Z	8	4	4	4
D_c/Mg m^{-3}	1.593	1.448	1.227	1.156
μ/mm^{-1}	1.204	0.862	0.526	0.533
F(000)	2264	1348	1804	1696
Wavelength/Å	0.71073	0.71073	0.71073	0.71073
Temperature/K	173(2)	173(2)	173(2)	173(2)
θ range for data collection/°	1.59 to 24.06	1.46 to 25.04	1.37 to 25.05	1.33 to 25.05
hkl ranges	−11,−10,−28 to 11,19,29	−10,0,0 to 9,15,33	−17,0,0 to 17,15,27	−18,0,0 to 18,11,37
Reflections collected	17822	14555	22049	21990
Independent reflections	3582 (R_{int} = 0.0402)	5183 (R_{int} = 0.0268)	7957 (R_{int} = 0.0467)	7839 (R_{int} = 0.0353)
Observed reflections [$I > 2\sigma(I)$]	3192	3866	5194	5405
Weighted scheme[a]	A = 0.042, B = 3.40	A = 0.0595, B = 4.7493	A = 0.0443, B = 1.9345	A = 0.0654, B = 0.5217
Absorption correction	Semi-empirical	SADABS	SADABS	SADABS
Max. and min. trans.	0.71391 and 0.56444	1.0000 and 0.8343	1.000 and 0.608	1.0000 and 0.7869
Data/restraints/parameters	3581/0/316	5183/4/366	7956/15/534	7836/32/487
Final R [$I > 2\sigma(I)$]	$R1$ = 0.0332, $wR2$ = 0.0804	$R1$ = 0.0586, $wR2$ = 0.1346	$R1$ = 0.0574, $wR2$ = 0.1082	$R1$ = 0.0514, $wR2$ = 0.1148
(all data)	$R1$ = 0.0391, $wR2$ = 0.0837	$R1$ = 0.0831, $wR2$ = 0.1469	$R1$ = 0.1049, $wR2$ = 0.1245	$R1$ = 0.0883, $wR2$ = 0.1306
G.o.f. on F^2	1.075	1.053	1.023	1.017
Largest difference peak and hole/e Å^{-3}	0.336 and −0.376	0.600 and −0.567	0.296 and −0.442	0.388 and −0.318

[a] $w = [\sigma^2(F_o^2) + (AP)^2 + (BP)]^{-1}$, where $P = (F_o^2 + 2F_c^2)/3$.

Table 2 Selected bond distances (Å) and angles (°) for crystallographically characterized compounds[a]

$[L^{Py}CuCl]PF_6$ (**1**)

Cu(1)—N(10)	2.038(2)	Cu(1)—N(1)	2.062(2)
Cu(1)—N(7)	2.137(2)	Cu(1)—N(4)	2.212(2)
Cu(1)—Cl(1)	2.2640(7)		
N(10)—Cu(1)—N(1)	81.93(8)	N(10)—Cu(1)—N(7)	148.92(8)
N(1)—Cu(1)—N(7)	83.65(8)	N(10)—Cu(1)—N(4)	118.96(8)
N(1)—Cu(1)—N(4)	83.74(8)	N(7)—Cu(1)—N(4)	86.45(8)
N(10)—Cu(1)—Cl(1)	95.28(6)	N(1)—Cu(1)—Cl(1)	176.51(6)
N(7)—Cu(1)—Cl(1)	99.79(6)	N(4)—Cu(1)—Cl(1)	95.85(5)

$\{L^{Py}Cu[Et_2N(N_2O_2)]\}PF_6$ (**2**)

Cu(1)—O(1)	1.955(3)	Cu(1)—O(2)	1.975(3)
Cu(1)—N(1)	2.047(3)	Cu(1)—N(4)	2.054(4)
Cu(1)—N(7)	2.323(3)	O(1)—N(1A)	1.297(5)
O(2)—N(2A)	1.321(4)	N(1A)—N(2A)	1.282(5)
N(2A)—N(3A)	1.448(6)		
O(1)—Cu(1)—O(2)	80.03(12)	O(1)—Cu(1)—N(1)	163.94(13)
O(2)—Cu(1)—N(1)	98.98(14)	O(1)—Cu(1)—N(4)	96.77(13)
O(2)—Cu(1)—N(4)	172.57(14)	N(1)—Cu(1)—N(4)	85.9(2)
O(1)—Cu(1)—N(7)	112.54(12)	O(2)—Cu(1)—N(7)	90.76(14)
N(1)—Cu(1)—N(7)	83.46(13)	N(4)—Cu(1)—N(7)	84.26(14)
N(1A)—O(1)—Cu(1)	115.0(2)	N(2A)—O(2)—Cu(1)	107.7(2)
N(2A)—N(1A)—O(1)	112.9(3)	N(1A)—N(2A)—O(2)	124.1(4)
N(1A)—N(2A)—N(3A)	117.6(4)	O(2)—N(2A)—N(3A)	118.3(4)

$\{L^{HAmH}Cu[Et_2N(N_2O_2)]\}BPh_4$ (**3**)

Cu(1)—O(2A)	1.951(2)	Cu(1)—O(1A)	1.964(2)
Cu(1)—N(7)	2.050(3)	Cu(1)—N(1)	2.061(3)
Cu(1)—N(4)	2.277(3)	O(1A)—N(1A)	1.308(4)
O(2A)—N(2A)	1.323(3)	N(1A)—N(2A)	1.285(4)
N(2A)—N(3A)	1.421(4)		
O(2A)—Cu(1)—O(1A)	80.25(10)	O(2A)—Cu(1)—N(7)	95.79(10)
O(1A)—Cu(1)—N(7)	174.35(11)	O(2A)—Cu(1)—N(1)	162.25(10)
O(1A)—Cu(1)—N(1)	98.99(10)	N(7)—Cu(1)—N(1)	86.01(11)
O(2A)—Cu(1)—N(4)	114.15(10)	O(1A)—Cu(1)—N(4)	92.48(10)
N(7)—Cu(1)—N(4)	85.43(10)	N(1)—Cu(1)—N(4)	83.59(10)
N(1A)—O(1A)—Cu(1)	113.8(2)	N(2A)—O(2A)—Cu(1)	107.6(2)
N(2A)—N(1A)—O(1A)	112.1(3)	N(1A)—N(2A)—O(2A)	124.2(3)
N(1A)—N(2A)—N(3A)	117.0(3)	O(2A)—N(2A)—N(3A)	118.8(3)

$\{L^{tBu2}Cu[Et_2N(N_2O_2)]\} \cdot 0.5C_5H_{12} \cdot C_6H_{12}O_2$ (**4** $\cdot 0.5C_5H_{12} \cdot C_6H_{12}O_2$)

Cu(1)—O(1)	1.916(3)	Cu(1)—O(2)	1.942(2)
Cu(1)—N(1)	2.047(2)	Cu(1)—N(3)	2.107(3)
Cu(1)—N(2)	2.321(3)	O(2)—N(4)	1.323(3)
O(3)—N(5)	1.289(3)	N(4)—N(5)	1.284(3)
N(5)—N(6)	1.436(3)		
O(1)—Cu(1)—O(2)	91.38(8)	O(1)—Cu(1)—N(1)	94.14(9)
O(2)—Cu(1)—N(1)	171.69(9)	O(1)—Cu(1)—N(3)	170.95(10)
O(2)—Cu(1)—N(3)	89.41(9)	N(1)—Cu(1)—N(3)	84.17(10)
O(1)—Cu(1)—N(2)	104.68(9)	O(2)—Cu(1)—N(2)	101.67(9)
N(1)—Cu(1)—N(2)	82.93(10)	N(3)—Cu(1)—N(2)	83.98(10)
N(4)—O(2)—Cu(1)	114.8(2)	N(5)—N(4)—O(2)	110.7(2)
N(4)—N(5)—O(3)	127.1(2)	N(4)—N(5)—N(6)	112.4(2)
O(3)—N(5)—N(6)	120.4(2)		

[a] Estimated standard deviations indicated in parentheses.

When necessary, solvents were dried according to published procedures and distilled under N_2 immediately prior to use. All air-sensitive reactions were performed either in a Vacuum Atmospheres inert-atmosphere glovebox under a N_2 atmosphere or by using standard Schlenk and vacuum line techniques. $Na[Et_2N(N_2O_2)]$,[3] L^{Py},[11] and $L^{R2}CuCl$ (R = Me or Bu^t)[12] were synthesized according to published procedures. L^{HAmH} was supplied by Dr. Lisa M. Berreau.[13] Elemental analyses were performed by Atlantic Microlabs of Norcross, GA. FTIR spectra were recorded on a Perkin Elmer 1600 Series FTIR spectrophotometer as KBr pellets. Electronic absorption spectra were recorded on a Hewlett-Packard HP8452A spectrophotometer (190–820 nm scan range) interfaced with a microcomputer for data acquisition and analysis. X-Band EPR spectra were recorded on a Bruker ESP300 spectrometer fitted with a liquid nitrogen finger dewar (77 K, $\approx$9.44 GHz). Electrospray ionization (ESI) mass spectral data were collected using a Sciex API III or Finnigan Triple Stage Quadrupole Electrospray Ionization Mass Spectrometer; fast atom bombardment (FAB) data were acquired using a VG

Table 3 Quantitation of nitric oxide (NO) release amounts and rates[a]

Compound (Solvent system)	% NO released[b]	0.1 M HCl		1.0 M HOAc		PBS Buffer	
		k_{obs}/s^{-1}	$t_{\frac{1}{2}}/s$	k_{obs}/s^{-1}	$t_{\frac{1}{2}}/s$	k_{obs}/s^{-1}	$t_{\frac{1}{2}}/s$
$Na[Et_2N(N_2O_2)]$ (10 mM NaOH)	80(3)	0.10(2) [0.043(4)][c]	6.9	0.11(1) [0.053(5)][c]	6.3	0.0033(4) [0.028(4)][c]	210
$Na[Et_2N(N_2O_2)]$	88(4)	0.10(1)	6.9	0.10(4)	6.9	0.0029(1)	239
$\{L^{iPr3}Cu[Et_2N(N_2O_2)]\}^+$ (MeOH, 10 mM OH^-)[d]	94(6)	0.083(3) [0.043(4)][c]	8.3	0.089(4) [0.022(3)][c]	7.8	0.0013(4) [0.012(1)][c]	533
$\{L^{iPr3}Cu[Et_2N(N_2O_2)]\}^+$	97(5)	0.086(7)	8.0	0.011(1)	63	0.0040(5)	173
2 (MeOH, 10 mM OH^-)[d]	90(2)	0.089(1)	7.8	0.094(3)	7.4	0.0031(1)	223
2	74(3)	0.13(1)	5.3	0.12(1)	5.8	0.0040(1)	173
3	92(2)	0.14(1)	4.9	0.13(1)	5.3	0.0073(9)	95
4 (R = Me)	59(4)	0.11(1)	6.3	0.12(1)	5.8	0.0032(2)	217
4 (R = Bu^t)	74(3)	0.091(9)	7.6	0.090(4)	7.7	0.0042(4)	165

[a] All experiments performed in MeOH solution unless indicated otherwise. See experimental section for details. [b] % based on release in 0.1 M HCl. [c] Data reported determined previously[7] using a different chemiluminescence instrument. [d] The complex was dissolved in minimal MeOH (≈20 μL) and diluted with 10 mM NaOH.

7070E-HF instrument. ESI samples were injected *via* syringe pump (20 μL min^{-1}) and spectra acquired using a 1 s scan time as described elsewhere.[19]

Preparations

$[L^{Py}CuCl]PF_6$ (1). A solution of L^{Py} (70 mg, 0.23 mmol) in CH_3OH (2 cm^3) was treated with a solution of anhydrous $CuCl_2$ (30 mg, 0.22 mmol) in CH_3OH (3 cm^3). The resultant blue solution was treated with an excess of NH_4PF_6 (0.50 g), causing the deposition of the product as blue microcrystals. Recrystallization from CH_2Cl_2–Et_2O afforded the pure product as blue needles (77 mg, 63%). Found: C, 39.42; H, 5.86; N, 10.15; $C_{18}H_{32}N_4F_6PClCu$ requires C, 39.42; H, 5.88; N, 10.22; λ_{max}/nm (CH_2Cl_2) 296 (ε/dm^3 mol^{-1} cm^{-1} 7100), 672 (170), 770 (170); ν/cm^{-1} 3092, 2980, 1609, 1492, 1387, 1307, 1175, 1069, 953, 837 (PF_6^-), 780, 559 (PF_6); EPR (1 : 1 CH_2Cl_2–toluene, 9.46 GHz, 77 K) $g_{\|} = 2.22$, $A_{\|}^{Cu} = 155 \times 10^{-4}$ cm^{-1}, $g_{\perp} = 2.03$; *m/z* (FAB, MBNA matrix) 402 (M − PF_6), 367 (M − Cl − PF_6). Crystals suitable for X-ray diffraction were obtained by diffusion of Et_2O into a solution of the complex in CH_3CN.

$\{L^{Py}Cu[Et_2N(N_2O_2)]\}PF_6$ (2). $Na[Et_2N(N_2O_2)]$ (127 mg, 0.820 mmol) was dissolved under nitrogen in dry, degassed MeOH (1 cm^3) and cooled to −45 °C. To this solution was added a solution of $[L^{Py}CuCl]PF_6$ (30 mg, 0.0547 mmol) in CH_2Cl_2 (1 cm^3) at −45 °C. As the mixture was stirred for 1 h at −45 °C, it changed from blue to green-blue. The solvent was removed under reduced pressure to yield a green-blue residue, which was dissolved in acetone (1–2 cm^3). Et_2O was allowed to diffuse into the solution at 4 °C, resulting in deposition of green clusters of crystalline product (0.0353 g, 69%). Found: C, 40.92; H, 6.29; N, 14.84; $C_{22}H_{42}CuF_6N_7O_2P$ requires C, 40.96; H, 6.56; N, 15.20; λ_{max}/nm (MeOH) 258 (ε/dm^3 mol^{-1} cm^{-1} 8000), 284 (4500), 670 (60); ν/cm^{-1} 2931, 1595, 1461, 1384, 1278, 1166, 1060, 941, 842 (PF_6^-), 562 (PF_6^-); EPR (1 : 1 CH_2Cl_2–toluene, 9.44 GHz, 77 K) $g_{\|} = 2.26$, $g_{\perp} = 2.06$, $A_{\|}^{Cu} = 161 \times 10^{-4}$ cm^{-1}.

$\{L^{HAmH}Cu[Et_2N(N_2O_2)]\}BPh_4$ (3). $CuCl_2$ (289 mg, 0.215 mmol) was dissolved under nitrogen in dry, degassed MeOH (3–4 cm^3) and cooled to −50 °C. To this solution was added a solution of $Na[Et_2N(N_2O_2)]$ (40 mg, 0.26 mmol) in MeOH (2 cm^3) cooled to −45 °C. As the mixture was stirred for 15 min, it changed from pale yellow-green to bright lime-green. L^{HAmH} (0.0702 g, 0.215 mmol) dissolved in MeOH (4 cm^3) was added dropwise to the reaction mixture. As the mixture was stirred for 15 min, it changed from bright lime-green to bright blue-green. After warming to −30 °C, a solution of $NaBPh_4$ (88 mg, 0.26 mmol) dissolved in MeOH (1 cm^3) was added dropwise to the reaction mixture to induce precipitation of a blue solid. Acetone (≈0.5 cm^3) was added until the precipitate just dissolved. Upon standing at −20 °C the product crystallized as green clusters (0.115 g, 64%). Found: C, 65.96; H, 8.02; N, 11.76; $C_{46}H_{68}BCuN_7O_3$ requires C, 65.66; H, 8.15; N, 11.65; λ_{max}/nm (MeOH) 228 (ε/dm^3 mol^{-1} cm^{-1} 24000), 266 (7800), 274 (6400), 288 (3900), 656 (40); ν/cm^{-1} 3372 (N—H), 3052, 2982, 2871, 1679 (C=O), 1529, 1477, 1548, 1378, 1293, 1264, 1216, 1202, 1174, 1131, 1063, 1035, 955, 934, 870, 844, 801, 736, 708, 610, 528, 505, 469; EPR (1 : 1 CH_2Cl_2–toluene, 9.44 GHz, 77 K) $g_{\|} = 2.26$, $g_{\perp} = 2.06$, $A_{\|}^{Cu} = 168 \times 10^{-4}$ cm^{-1}; *m/z* (ESI, acetone) 521 (M − BPh_4), 389 [M − $(Et_2N)N_2O_2$ − BPh_4]. Crystals suitable for X-ray crystallography were grown from acetone–Et_2O.

$\{L^{Me2}Cu[Et_2N(N_2O_2)]\}$ (4, R = Me). To a solution of $L^{Me2}CuCl$ (60 mg, 0.135 mmol) dissolved under nitrogen in dry, degassed MeOH (2–3 cm^3) at −30 °C was added a solution of $Na[Et_2N(N_2O_2)]$ (31 mg, 0.20 mmol) in MeOH (2 cm^3) at −30 °C. As the mixture was stirred for ≈30 min at −30 °C, it changed from dark purple to brown. The solvent was removed under reduced pressure, the brown residue was dissolved in acetone (3 cm^3) that had been predried over 4 Å molecular sieves, and pentane was allowed to diffuse in at −20 °C. After ≈1–2 days, a tan precipitate formed, which was removed *via* filtration through a celite. Subsequent diffusion of pentane into the filtrate at −20 °C led to the deposition of the product as brown crystals (0.023 g, 38%). Found: C, 53.35; H, 8.66; N, 13.45; $C_{25}H_{46}N_6CuO_3 \cdot (CH_3OH)_2$ requires C, 53.49; H, 8.98; N, 13.86; the presence of the MeOH solvate is corroborated by FTIR; λ_{max}/nm (MeOH) 242 (ε/dm^3 mol^{-1} cm^{-1} 10 800), 282 (5600), 496 (640), 668 (sh), (160); ν/cm^{-1} 3417 (MeOH), 2968, 2912, 1712, 1473, 1389, 1325, 1270, 1164, 1059, 974, 863, 800, 764; EPR (1 : 1 MeOH–toluene, 9.44 GHz, 77 K) $g_{\|} = 2.26$, $g_{\perp} = 2.05$, $A_{\|}^{Cu} = 160 \times 10^{-4}$ cm^{-1}; *m/z* (ESI, MeOH) 542 ([M + H]$^+$, 7), 389 ([$L^{Me2}Cu$], 100).

$\{L^{tBu2}Cu[Et_2N(N_2O_2)]\}$ (4, R = Bu^t). Method A: $L^{tBu2}CuCl$ (0.051 g, 0.096 mmol) was dissolved in dry, degassed methanol (2 cm^3). A similar solution of $Na[Et_2N(N_2O_2)]$ (0.0224 g, 0.144 mmol) in MeOH (2 cm^3) cooled to −30 °C was added to the purple copper solution. The solution immediately turned brown and was stirred for 1 h at −30 °C. The solvent was removed under reduced pres-

sure. The resultant brown residue was dissolved in acetone (2 cm^3) that had been predried over 4 Å molecular sieves. Pentane was diffused into this solution at −20 °C. The brown solution was separated from a white solid that had precipitated overnight. Pentane (≈10 cm^3) was gently layered on the brown solution. After about 1 week at −20 °C, X-ray quality crystals deposited. Method B: $Na[Et_2N(N_2O_2)]$ (0.0627 g, 0.404 mmol) was dissolved in acetone (2 cm^3) that had been predried over 4 Å molecular sieves. A similar solution of $L^{tBu2}CuCl$ (0.214 g, 0.404 mmol) in acetone (4 cm^3) cooled to −50 °C was added to the $Na[Et_2N(N_2O_2)]$ solution. The solution immediately turned brown and was stirred for 30 min at −50 °C before concentrating the solution under reduced pressure to 1–2 cm^3. The mixture was filtered through celite and the remaining solid was washed with acetone (1–2 cm^3). The brown filtrate was concentrated to ≈1 cm^3. Pentane (3 cm^3) was layered on the solution, which was subsequently placed in a −20 °C freezer. The brown filtrate was separated from a brown and purple solid that precipitated after 4–5 days. The filtrate was concentrated to dryness. The brown powder was redissolved in THF (1 cm^3) and layered with pentane (3.5 cm^3). After about 1 week, crystals deposited at the edge of the solution (≈5 mg). Large quantities of material were not obtained with either method. λ_{max}/nm (MeOH) 244 (ε/dm^3 mol^{-1} cm^{-1}12 000), 284 (7300), 322 (3500), 518 (900), 686 (300); ν/cm^{-1} 3449 ($C_6H_{12}O_2$), 2963, 2862, 1624, 1469, 1416, 1388, 1371, 1316, 1295, 1243, 1173, 1133, 1107, 1082, 1071; EPR (1 : 1 MeOH–toluene, 9.44 GHz, 77 K) $g_{\|} = 2.25$, $g_{\perp} = 2.04$, $A_{\|}^{Cu} = 179 \times 10^{-4}$ cm^{-1}; *m/z* (ESI, MeOH) 626 ($[M + H]^+$, 32), 493 ($[L^{tBu2}Cu]$, 100).

Analysis of NO evolution

The compounds were tested for NO release under various conditions using a Sievers 280 Chemiluminescence Nitric Oxide Analyzer. The chemiluminescence due to the decay of the product of the trapping of NO with O_3 is converted into a mV signal that is plotted *versus* time. The correspondence of the signal to the moles of NO was obtained by calibration using a 2.0 mM PBS buffer (pH 7.4) solution of $NaNO_2$. For a typical calibration, a solution of 1 : 1 : 0.1 M HCl–0.56 M KI (1.5 cm^3) was added to a 3 cm^3 reaction vial, and it was sealed with a open-top cap adapted with a teflon-rubber-sealed septum. A stainless steel needle with a positive flow of nitrogen was inserted into the vial along with a second needle that was connected to the instrument. The solution was purged with nitrogen and equilibrated at 37 °C for 4–6 min. Measured additions of the $NaNO_2$ solution were then added to the vial *via* a gas-tight syringe. The area under the chemiluminescence signal curve was determined for each incremental injection. Since $NaNO_2$ releases NO in a 1 : 1 stoichiometry and the amount injected was known, the observed areas can be directly correlated to the nmols of NO being introduced into the instrument. A plot of area under the curve *versus* nmols of NO was shown to be linear in the 10–70 nmol range. This plot was then used to determine the amount of NO released from the compounds of interest. The NO release profile for the compounds was obtained by injecting 30 μL of a stock solution of each species into a degassed solution at 37 °C that contained 0.1 HCl, 1.0 M HOAc or PBS buffer (pH 7.4). The stock solutions prepared with the indicated solvent system ranged from 0.60–2.6 mM. Table 3 lists the median percent of NO released from the compounds after injection into 0.1 M HCl for at least three replicate trials based on two mols of NO per mol of compound. The standard deviations indicated in parentheses were estimated from the variance in the trials. The rate constants for NO release were obtained by plotting the area under the chemiluminescence response curve *versus* time and fitting the exponential using the KaleidaGraph program. The exponential was fit ($R \geqslant 0.988$) over at least two half-lives. Rate constants listed in Table 3 are the median k_{obs} from at least three replicate trials; the standard deviations indicated in parentheses were estimated from the variance in the trials.

Crystallography

Data collection. Single crystals of $[L^{Py}CuCl]PF_6$ (**1**, 0.50 × 0.45 × 0.24 mm), $\{L^{Py}Cu[Et_2N(N_2O_2)]\}PF_6$ (**2**, 0.45 × 0.25 × 0.22 mm), $\{L^{HAmH}Cu[Et_2N(N_2O_2)]\}BPh_4$ (**3**, 0.48 × 0.38 × 0.06 mm) and $\{L^{tBu2}Cu[Et_2N(N_2O_2)]\}\cdot 0.5C_5H_{12}\cdot C_6H_{12}O_2$ (**4**, $0.5C_5H_{12}\cdot C_6H_{12}O_2$, 0.46 × 0.35 × 0.06 mm) were attached to glass fibers and mounted on the Siemens SMART system for data collection at 173(2) K. Initial sets of cell constants were calculated from reflections harvested from three sets of 20–30 frames oriented such that orthogonal wedges of reciprocal space were surveyed. Final cell constants were calculated from 8192, 6462, 8192 or 7679 strong reflections, respectively, from the actual data collection. Data were collected *via* the hemisphere collection method, whereby a randomly oriented region of reciprocal space was surveyed to the extent of 1.3 hemispheres to a resolution of 0.87 Å. Three major swaths of frames with 0.30° steps in ω were collected. Crystallographic data and experimental details for all of the structures are listed in Table 1.

Structure solution and refinement. For each structure, a successful direct-methods solution was calculated that provided most non-hydrogen atoms from the E-map. Several full-matrix least squares/difference Fourier cycles were performed to locate the remainder of the non-hydrogen atoms. All non-hydrogen atoms were refined with anisotropic displacement parameters, and all hydrogen atoms (except where noted below) were placed in ideal positions and refined as riding atoms with individual (or group, if appropriate) isotropic displacement parameters. All calculations were performed using SGI INDY R4400-SC or Pentium computers using the SHELXTL V5.0 suit of programs.[20]

In the cases of **2** and **3**, one ethyl group of the $[Et_2N(N_2O_2)]^-$ ligand was found to be disordered over two positions, with respective occupancies of 0.59(1) [C(25)—C(26)]/0.41(1) [C(25′)—C(26′)] and 0.80(1) [C(24)—C(25)]/0.20(1) [C24′)—C(25′)]. Constraints were applied to the C—C bond lengths and the anisotropic displacement parameters for each atom in the disordered group. In the latter structure, the amido H atom (H10) was located and refined anisotropically.

In the case of $\mathbf{4}\cdot 0.5C_5H_{12}\cdot C_6H_{12}O_2$, the asymmetric unit was found to contain a half molecule of pentane disordered near an inversion center and an unexpected molecule assigned as the aldol condensation product $C_6H_{12}O_2$ of acetone that was used during the crystallization. This assignment is based on the reasonable bond distances and angles within the molecule and the acceptable displacement parameters of the atoms. A total of 32 restraints (SIMU, DELU, DFIX) were applied to the two solvent molecules (see Supporting Information).

CCDC reference number 440/025.

Acknowledgements

Financial support for this research was provided by the National Institutes of Health (GM47365), the National Science Foundation (National Young Investigator Award to WBT), the Camille & Henry Dreyfus and Sloan Foundations (fellowships to WBT), Unilever Corporation, and Comedicus Corporation. We thank Christine Brinkman and Professor Daniel Mooradian for their assistance with the chemiluminescence detection experiments and Dr. Lisa Berreau for providing L^{HAmH}.

References

1 *The Biology of Nitric Oxide, Part 5*, eds. S. Moncada, J. Stamler, S. Gross and E. A. Higgs, Portland Press, London, 1996, and preceeding volumes.

2 J. T. Groves and S. S. Marla, *J. Am. Chem. Soc.*, 1995, **117**, 9578 and references cited therein; W. A. Pryor, X. Jin and G. L. Squadrito, *J. Am. Chem. Soc.*, 1996, **118**, 3125 and references cited therein; D. S. Bohle, B. Hansert, S. C. Paulson and B. D. Smith, *J. Am. Chem. Soc.*, 1994, **116**, 7423; S. Goldstein, G. L. Squadrito, W. A. Pryor and G. Czapski, *Free Radical Biol. Med.*, 1996, **21**, 965 and references cited therein.

3 R. S. Drago and F. E. Paulik, *J. Am. Chem. Soc.*, 1960, **82**, 96; R. S. Drago and B. R. Karstetter, *J. Am. Chem. Soc.*, 1961, **83**, 1819; J. A. Hrabie, J. R. Klose, D. A. Wink and L. K. Keefer, *J. Org. Chem.*, 1993, **58**, 1472.

4 C. M. Maragos, D. Morley, D. A. Wink, T. M. Dunams, J. E. Saavedra, A. Hoffman, A. A. Bove, L. Isaac, J. A. Hrabie and L. K. Keefer, *J. Med. Chem.*, 1991, **34**, 3242; C. M. Maragos, J. M. Wang, J. A. Hrabie, J. J. Oppenheim and L. K. Keefer, *Cancer Res.*, 1993, **53**, 564; J. G. Diodati, A. A. Quyyumi, N. Hussain and L. K. Keefer, *Thromb. Haem.*, 1993, **70**, 654; D. L. Mooradian, T. C. Hutsell and L. K. Keefer, *J. Cardiovas. Pharmacol.*, 1995, **25**, 674; D. A. Wink, L. Hanbauer, M. C. Krishna, W. DeGraff, J. Gamson and J. B. Mitchell, *Proc. Natl. Acad. Sci. USA*, 1993, **90**, 9813; J. E. Saavedra, T. R. Billiar, D. L. Williams, Y.-M. Kim, S. C. Watkins and L. K. Keefer, *J. Med. Chem.*, 1997, **40**, 1947.

5 J. E. Saavedra, T. M. Dunams, J. L. Flippen-Anderson and L. K. Keefer, *J. Org. Chem.*, 1992, **57**, 6134.

6 D. Christodoulou, C. George and L. K. Keefer, *J. Chem. Soc., Chem. Commun.*, 1993, 937; D. Christodoulou, C. M. Maragos, C. George, D. Morley, T. M. Dunams, D. A. Wink and L. K. Keefer, in *Bioinorganic Chemistry of Copper*, eds. K. D. Karlin and Z. Tyeklár, Chapman & Hall, New York, 1993, pp. 427–436; D. Christodoulou, D. Wink, C. F. George, J. E. Saavedra and L. K. Keefer, in *Nitrosomine and Related* N-*Nitroso Compounds*, eds. R. N. Loeppky and C. J. Michejda, ACS Symposium Series 553, American Chemical Society, Washington, D. C. 1994, pp. 307–308; D. D. Christodoulou, D. A. Wink, Jr. and L. K. Keefer, *US Patent*, 5 389, 675, 1995.

7 J. L. Schneider, V. G. Young, Jr. and W. B. Tolman, *Inorg. Chem.*, 1996, **35**, 5410.

8 R = alkyl: S. R. Fletcher and A. C. Skapski, *J. Organomet. Chem.*, 1973, **59**, 299; J. D. Wilkins and M. G. B. Drew, *J. Organomet. Chem.*, 1974, **69**, 111; P. Edwards, K. Mertis, G. Wilkinson, M. B. Hursthouse and K. M. A. Malik, *J. Chem. Soc., Dalton Trans.*, 1980, 334; G. Fochi, C. Floriani, A. Chiesi-Villa and C. Guastini, *J. Chem. Soc., Dalton Trans.*, 1986, 445; M. H. Abraham, J. I. Bullock, J. H. N. Garland, A. J. Golder, G. J. Harden, L. F. Larkworthy, D. C. Povey, M. J. Riedl and G. W. Smith, *Polyhedron*, 1987, **6**, 1375; S. V. Evans, P. Legzdins, S. J. Rettig, L. Sánchez and J. Trotter, *Acta Crystallogr., Sect. C*, 1995, **51**, 584.

9 R = Ph (cupferron): D van der Helm, L. L. Merritt, Jr., R. Degeilh and C. H. MacGillavry, *Acta Crystallogr.*, 1965, **18**, 355; J. Charalambous, L. I. B. Haines, N. J. Harris, K. Henrick and F. B. Taylor, *J. Chem. Res.* (*S*), 1984, 220; S. S. Basson, J. G. Leipoldt, A. Roodt and J. A. Venter, *Inorg. Chim. Acta*, 1986, **118**, L45; S. S. Basson, J. G. Leipoldt and J. A. Venter, *Inorg. Chim. Acta*, 1987, **128**, 31; S. S. Basson, J. G. Leipoldt and J. A. Venter, *Acta Crystallogr., Sect. C*, 1990, **46**, 1324; S. S. Basson, J. G. Leipoldt, W. Purcell and J. A. Venter, *Acta Crystallogr., Sect. C*, 1992, **48**, 171; N. Okabe and K. Tamaki, *Acta Crystallogr., Sect. C*, 1995, **51**, 2004; Y. Elerman, O. Atakol, I. Svoboda and M. Geselle, *Acta Crystallogr., Sect. C*, 1995, **51**, 1520.

10 G.-B. Yi, M. A. Khan and G. R. Richter-Addo, *Inorg. Chem.*, 1995, **34**, 5703.

11 J. A. Halfen, V. G. Young, Jr. and W. B. Tolman, *J. Am. Chem. Soc.*, 1996, **118**, 10920.

12 J. A. Halfen, B. A. Jazdzewski, S. Mahapatra, L. M. Berreau, E. C. Wilkinson, L. Que, Jr. and W. B. Tolman, *J. Am. Chem. Soc.*, 1997, **119**, 8217; J. A. Halfen, V. G. Young, Jr. and W. B. Tolman, *Angew. Chem., Int. Ed. Engl.*, 1996, **35**, 1687.

13 L. M. Berreau, J. A. Halfen, V. G. Young, Jr. and W. B. Tolman, *Inorg. Chem.*, 1998, **37**, 1091.

14 A. W. Addison, T. N. Rao, J. Reedjik, J. von Rijn and G. C. Verschoor, *J. Chem. Soc., Dalton Trans.*, 1984, 1349.

15 N. Wei, N. N. Murthy and K. D. Karlin, *Inorg. Chem.*, 1994, **33**, 6093.

16 PBS buffer = 0.27 M KCl, 0.014 M NaCl, 1.1 mM Na_2HPO_4 and 0.15 mM KH_2PO_4.

17 S. L. Archer, P. J. Shultz, J. B. Warren, V. Hampl and E. G. DeMaster, *Comp. Methods Enzymol.*, 1996, **7**, 21.

18 We previously stated[7] that the rate of release of NO from $\{L^{iPr3}Cu[Et_2N(N_2O_2)]\}O_3SCF_3$ under acidic conditions (1.0 M HOAc) was $\approx$2 times slower than the parent $Na[Et_2N(N_2O_2)]$, but remeasurement using the more sensitive instrumentation confirmed that the rates were essentially the same when NaOH was pre-added. However, our previous conclusions regarding the $\approx$two-fold difference in rate in PBS buffer, where differences between the two instruments are alleviated because of the slower rates, remain unchanged.

19 J. Kim, Y. Dong, E. Larka and L. Que, Jr. *Inorg. Chem.*, 1996, **35**, 2369; D. M. Garcia, S. K. Huang and W. F. Stansbury, *J. Am. Soc., Mass Spectrom.*, 1996, **7**, 59–65.

20 SHELXTL V5.0, Seimens Energy & Automation, Inc., Madison, WI 53719-1173.

Received in New Haven, CT, USA, 19th January 1998;
Paper 8/00561/C